Molecular Interactions of Danofloxacin with Bovine Serum Albumin: An Experimental and Theoretical Investigation

Masoomeh Shaghaghi[1*], Samaneh Rashtbari[2], Laleh Solouki[1], Somaieh Soltani[3,4], Gholamreza Dehghan[2]

1. Department of Chemistry, Payame Noor University, P. O. Box 19395-4697 Tehran, Iran
2. Department of Biology, Faculty of Natural Sciences, University of Tabriz, Tabriz, Iran
3. Pharmaceutical Analysis Research Center, Tabriz University of Medical Sciences, Tabriz, Iran
4. Pharmacy Faculty, Tabriz University of Medical Sciences, Tabriz, Iran

Abstract

Danofloxacin (DNF), a synthetic fluoroquinolone, is widely used as an antibacterial agent against a broad spectrum of pathogens. In the present study, the effects of DNF on the structure of bovine serum albumin (BSA) were investigated using UV-Vis absorption and fluorescence spectroscopy, and molecular docking methods at different temperatures. The obtained results of UV-Vis absorption studies showed that the microenvironment of the fluorophore residues does not significantly change upon interaction with DNF. Also, fluorometric studies revealed BSA-DNF complex formation and fluorescence quenching of BSA in the presence of DNF. The number of binding sites and binding constants were calculated to be ~1 and in the order of 10^3, respectively. According to thermodynamic parameters, van der Waals forces and hydrogen bonding play the main role in the BSA-DNF complex formation, which is a spontaneous process. The binding distance between DNF and BSA was calculated by the Förster resonance energy transfer (FRET) method. Molecular docking results were in agreement with thermodynamic and spectroscopic data and confirmed the binding mechanism of DNF to BSA.

1. INTRODUCTION

Serum albumin is the most abundant protein in the circulatory system, accounting for 55 percent of total protein in the blood. The amino acid sequences of human serum albumin (HSA) and bovine serum albumin (BSA) are 76 percent same and 87 percent comparable [1-4]. BSA is used as a biological model in bioanalytical and biochemical studies to investigate the molecular interaction pattern of various drugs with serum albumins (protein-protein and protein-drug interaction). Due to the significant similarity of BSA and HSA, low cost, and availability, BSA is also used to study the pharmacokinetic and pharmacodynamic features of different medications in the body to better understand the metabolism and transport process of drugs [5-7]. As a result, drug-protein binding (interaction) studies are a hot topic in clinical medicine, chemistry, and biology, and can aid in the development of new drugs with effective therapy. It's also critical to look at how different ligands affect the activity and structure of these proteins. BSA has a predominantly α-helical structure. It contains 583 amino acid residues, 35 cysteines (17 disulfide bridges), and three similar structure domains which are named I, II, and III. Each domain is divided into two subdomains, A and B [8-11]. Serum albumin takes part in many important physiological activities including maintaining the osmotic pressure of plasma, binding to various small exogenous and endogenous molecules such as fatty acids, amino acids, hormones, drugs, etc., and transporting these compounds in the circulatory system [12-14]. Sites I and II, which are situated in subdomains IIA and IIIA, respectively, are critical for BSA's ligand binding capacity and are BSA's two principal binding sites [5, 8, 15, 16].

Danofloxacin (DNF; Fig. 1), a synthetic fluoroquinolone, is commonly employed as an antibacterial agent against both gram-negative and gram-positive infections. The mechanism of antibacterial activity of DNF is through the internalization via bacterial porin protein and inhibition of DNA gyrase which can result in the disruption of bacterial DNA replication [17-20].

*Corresponding Author: m.shag2003d@yahoo.com and m_shaghaghi@pnu.ac.ir
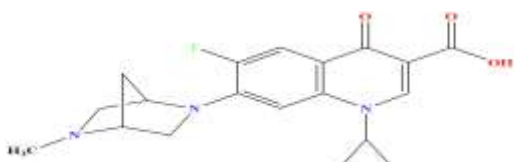
Fig. 1. Chemical structure of DNF.

In recent years, optical techniques, particularly fluorescence spectroscopy, as valuable tools owing to their high sensitivity, selectivity, rapidity, and abundant theoretical foundation are extensively used to explore the binding features of various small molecules (ligands or medicines) to some proteins, together with the molecular docking simulation method [3, 6]. In the present study, UV-Vis absorption and fluorescence emission spectroscopy were used to investigate the number of binding sites (n), binding constants (K_b), major binding forces, and structural and conformational changes of BSA following DNF binding. The molecular docking simulation was used to explore the exact mechanism of DNF binding to BSA.

2. EXPERIMENTAL
2.1. Materials
Fatty-acid free BSA (<0.05%) was obtained from Sigma-Aldrich Co. (St. Louis, MO, USA). By dissolving the appropriate amount (3.152 g) of Tris-HCl powder, a 0.2 M Tris-HCl buffer solution (Merck Co., Darmstadt, Germany) was created in 100 mL double distilled water, and the pH of the prepared solution was adjusted to 7.5 using HCl or NaOH (Merck Co., Darmstadt, Germany). A stock solution of BSA (5.0×10^{-5} M) was prepared by dissolving a 0.3 g BSA crystalline powder in 100 mL Tris-HCl buffer solution and was stored at 4.0 °C. A 0.01 M DNF (Rooyan Darou Pharmaceutical Co., Tehran, Iran) stock solution was prepared by dissolving a 0.089 g DNF powder in a 50% (v/v) solution of water-methanol (25 mL).

2.2. Apparatus and Methods
All UV-Vis absorption spectra of BSA (10×10^{-6} M) in the presence and absence of various concentrations of DNF [$(0-100)\times10^{-6}$ M] were recorded on a UV–Vis spectrophotometer (T60, PG Instruments Ltd, Leicestershire, UK) with 1.0 cm path length quartz cuvette in the range of 200-400 nm at 298 K.
The fluorescence spectra of BSA (10×10^{-6} M) without and with extra concentrations of DNF [$(0-100)\times10^{-6}$ M] were recorded using a Jasco FP-750 spectrofluorimeter (Kyoto, Japan), at three temperatures 288, 298, and 310 K. Excitation of prepared materials was done at 280 nm (ex = 280 nm), and emission spectra were scanned in the 300-500 nm region.
To further investigate the interaction between BSA and DNF and determine the possible binding site

of DNF on BSA, molecular docking studies were carried out using AutoDock 4.2 software. The crystal structure of DNF was downloaded from the PubChem (CID: 71335) in SDF format and the 3D structure of BSA (PDB accession number 3V03) was obtained from the protein data bank (PDB; http://www.rcsb.org) in PDB format. GaussView 5.0 software was used to optimize the energy of DNF at the theoretical level of B3LYP with a 6–31G basis set. BSA contains two identical subdomains (A and B), so, in docking studies, only one chain (chain A) was selected as a target molecule. The water molecules were removed from the protein structure, and the only polar hydrogen atoms and Kollman partial charges. Firstly, to determine the potential binding site of DNF on BSA, blind dockings were completed using a grid size of 126×126×126 Å. Then, using a grid size of 90×90×90 Å, the lowest docked conformation was chosen for the following investigations. Finally, the outputs were analyzed by UCSF Chimera and Discovery Studio Client 4.1 programs.

3. RESULT AND DISCUSSION
3.1. Binding studies using molecular absorption (UV-Vis) spectroscopy
The effects of DNF on the structure of BSA were investigated using UV-Vis absorption spectroscopy. This method is commonly used to explore the structural changes of proteins in response to ligand interaction and the formation of protein-ligand complexes [16, 21]. Due to the presence of aromatic amino acids (Trp, Tyr, and Phe), BSA's absorption spectrum exhibits a maximum peak at 280 nm and π-π^* transitions of the carbonyl groups of these amino acids (especially Trp) [16, 22, 23]. Fig. 2A shows the changes in the absorption spectra of BSA upon interaction with different concentrations of DNF.
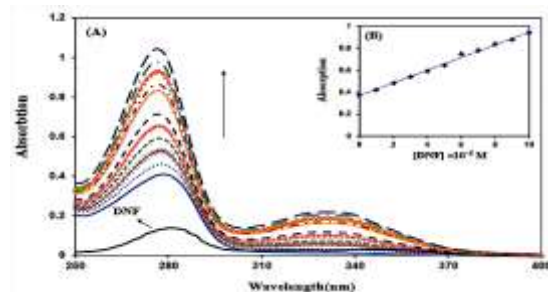
Fig. 2. (A) UV-Vis absorption spectra of BSA in the presence of various DNF concentrations and (B) the changes in BSA absorption after the addition of an increasing concentration of DNF; [BSA] = 10×10^{-6} M, [DNF] = $(0-100)\times10^{-6}$ M (from a to k), pH 7.4 and T = 298 K.

It is obvious that the absorption spectra of BSA continuously increase in the presence of additional concentrations of DNF without any noticeable

shift. More investigations revealed that DNF has its absorption at 280 nm (maximum absorption of BSA). However, a considerable increase in the absorption spectra of BSA was observed after subtracting the DNF absorption from the maximum absorption of BSA (Fig. 2B). These results confirmed BSA-DNF complex formation and showed that the microenvironment of the fluorophore residues does not change significantly upon interaction with DNF [22].

3.2. Quenching mechanism and thermodynamic analysis of BSA induced by DNF

Fluorescence spectroscopy is a simple and sensitive method that is widely used for studying the fluorescence of proteins and finding the main information of different parameters, for protein-ligand interaction including the binding site, binding mechanism, and strength of binding [24, 25]. The intrinsic emission intensity of proteins arises from the existence of main aromatic residues (Trp, Tyr, and Phe) in their structure [26, 27]. Various exogenous substances can change the intrinsic fluorescence of proteins and produce main information about their folding and structure [4, 28]. The fluorescence emission spectra of the BSA are shown in Fig. 3. The emission intensity of BSA at 347 nm decreases continuously in the presence of additional concentrations of DNF with a significant redshift (from 347 nm to 354 nm). These results confirmed BSA-DNF complex formation and fluorescence quenching of BSA with increasing DNF in its solution as well as the alteration of protein tertiary structure [11, 16, 29]. Also, the isosbestic point was found at 384 nm indicating the fluorescence quenching of NF and BSA. The following equation (Eq. 1) was used to compute the Stern-Volmer constants and estimate the emission quenching mechanism of BSA in the presence of DNF [26, 30, 31]:

$$\frac{F_0}{F} = 1 + K_{SV}[Q] = 1 + k_q \tau_0 [Q] \qquad (1)$$

where F_0 and F are the emission intensities of BSA without and with DNF, respectively; *[Q]* is the DNF concentration (M); K_{sv} (M^{-1}), k_q (M^{-1}s^{-1}), and τ_0 (10^{-8} s) are the Stern-Volmer quenching constant, biomolecule quenching rate constant, and average fluorescence lifespan of BSA without DNF, respectively. Fig. 4 shows the plots of F_0/F against additional concentrations of DNF for three different temperatures. According to these plots, the values of K_{SV} and k_q were calculated and the

results are shown in Table 1. It is clear from Table 1 that K_{sv} and k_q values decrease with increasing temperature, and k_q values are significantly higher than 2.0×10^{10} M^{-1}s^{-1}, the maximum dynamic quenching constant, indicating a static quenching mechanism of BSA upon interaction with DNF [3]. In general, there are two types of emission quenching mechanisms between a fluorophore and a quencher which are temperature-dependent processes: the dynamic and static mechanisms of quenching. In the dynamic mechanism, the values of K_{SV} increase as the temperature increase while in the static mechanism the values of the K_{SV} decrease as the temperature increase. Dynamic quenching is caused by a collision between the fluorophore's excited state and the quencher, whereas static quenching is caused by the construction of a ground-state complex between the fluorophore and the quencher [3, 6, 32, 33].
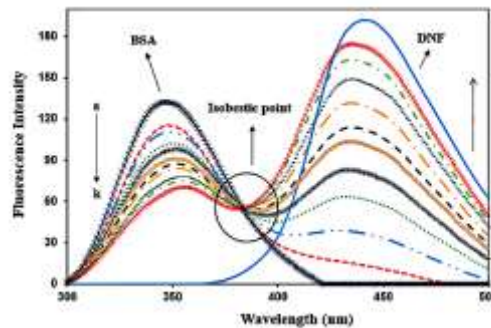
Fig. 3. The steady-state fluorescence spectra of BSA in the presence of additional concentrations of DNF; [BSA] = 10×10^{-6} M, [DNF] = $(0-100) \times 10^{-6}$ M, pH 7.4, λ_{ex} = 280 nm and T = 298 K.
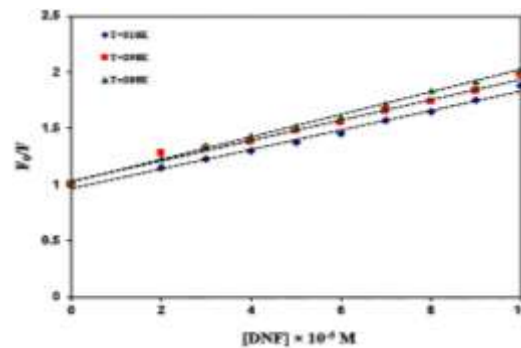
Fig. 4. Stern-Volmer plots for BSA interaction with DNF at three different temperatures; [BSA] = 10×10^{-6} M, [DNF] = $(0-100) \times 10^{-6}$ M, pH 7.4 and T = 298, 288 and 310 K.

**Table 1.** Calculated Stern–Volmer quenching and effective quenching constants for interactions of BSA with DNF.

T (°K)	K_{SV} ($\times 10^4$ M^{-1})	k_q ($\times 10^{12}$ M^{-1}s^{-1})	SD	R^2	K_a ($\times 10^4$ M^{-1})	SD	R^2
288	0.999	0.999	0.0032	0.9974	1.55	0.0020	0.9967
298	0.903	0.903	0.0036	0.9881	1.14	0.0024	0.9854
310	0.841	0.841	0.0032	0.9922	0.07	0.0073	0.9875

R^2 is the correlation coefficient for Stern-Volmer plots; SD corresponds to the standard deviation (three measurements) for the K_{sv} and K_a values.

Data of fluorescence quenching were further analyzed using a modified Stern-Volmer equation (Eq. 2):

$$\frac{F_0}{\Delta F} = \frac{1}{f_a K_a} \cdot \frac{1}{[Q]} + \frac{1}{f_a}$$
(2)

where, f_a and K_a (M^{-1}) represent the fraction of accessible fluorescence and the effective quenching constant for the accessible BSA, respectively. Fig. 5 and Table 1 show modified Stern–Volmer plots for three different temperatures and relevant results, respectively. The results indicated that the values of K_a decrease with increasing temperature, which further confirmed the static quenching mechanism of BSA-DNF [3, 29].
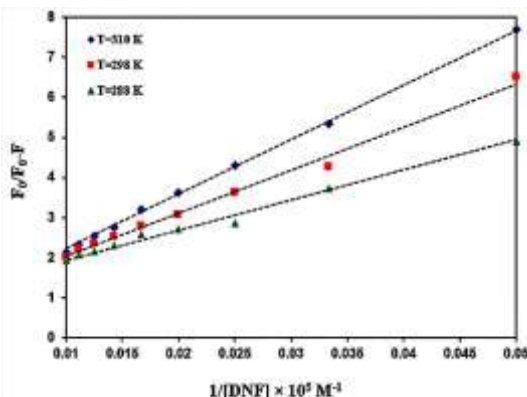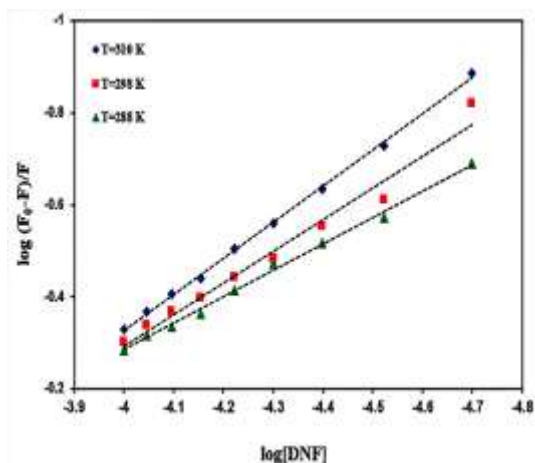

Fig. 5. Modified Stern-Volmer plots for quenching of BSA upon interaction with DNF at three different temperatures; [BSA] = 10×10^{-6} M, [DNF] = (0-100)×10^{-6} M, pH 7.4 and T = 298, 288 and 310 K.

On the other hand, the double logarithmic regression equation (Eq. 3) was applied for the calculation of K_b (M^{-1}) and n values of binding of DNF to BSA.

$$\log \frac{F_0 - F}{F} = \log K_b + n \log[Q]$$
(3)

The n and K_b denote the Hill coefficient (number of binding sites) and the binding constant, respectively. Fig. 6 shows double logarithm plots (log (F$_0$-F/F) versus log [Q] plots) and Table 2 represents the obtained values. The n values were approximately 1, indicating only one binding site of DNF on the BSA structure. The K_b values of the BSA with DNF were distributed in the range of 10^3, indicating considerable binding potency of DNF and this compound can tightly bind to BSA.

Fig. 6. Double logarithmic regression plots for quenching of BSA in the presence of DNF at three different temperatures; [BSA] = 10×10^{-6} M, [DNF] = (0-100)×10^{-6} M, pH 7.4 and T = 298, 288 and 310 K.

Meanwhile, thermodynamic parameters were calculated using the following equations (Eq. 4 and 5) for further understanding of the interaction process and the calculated values are presented in Table 2.

$$\ln K = -\frac{\Delta H}{RT} + \frac{\Delta S}{R}$$
(4)

$$\Delta G = \Delta H - T\Delta S$$
(5)

where K denotes the equilibrium constant (M^{-1}); R and T represent the universal gas constant (with a value of 8.314 J.mol^{-1}K^{-1}) and temperature (K), respectively. Generally, thermodynamic parameters ΔS (J.mol^{-1}K^{-1}), ΔH (KJ.mol^{-1}), and ΔG (KJ.mol^{-1}) (entropy, enthalpy, and the Gibbs free energy changes, respectively) are used to determine the binding modes including van der Waals forces ($\Delta H<0$ and $\Delta S<0$), electrostatic interactions ($\Delta H<0$ and $\Delta S>0$), hydrogen bonds ($\Delta H<0$ and $\Delta S<0$) and hydrophobic interactions ($\Delta H>0$ and $\Delta S>0$) [23]. The plot of lnK against 1/T was depicted in Fig. 7. As shown in this figure, the linear regression curve was as y = 3055.9x - 0.9472 (R^2 = 0.977). The slope and the intercept of this plot were used to determine ΔH and ΔS values, respectively. The corresponding values of thermodynamic parameters are shown in Table 2. According to this table, the negative values of ΔH and ΔS showed van der Waals forces and electrostatic interactions main role during the interaction process between BSA and DNF.

Table 2. Calculated thermodynamics parameters for interactions of BSA with DNF.

T (K)	ΔG (KJ.mol^{-1})	ΔH (KJ.mol^{-1})	ΔS (J. K^{-1}mol^{-1})	n	K$_b$ (×10^3 M^{-1})
288	-27.67			0.90	3.85
298	-27.75	-25.40	-7.78	0.82	1.83
310	-27.84			0.78	0.24

SD corresponds to the standard deviation (three measurements) for the K_b values.
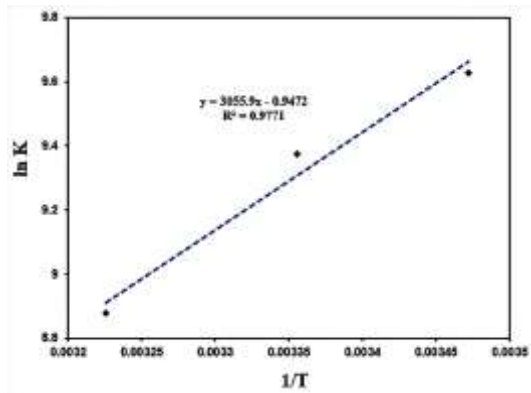
Fig. 7. The van't Hoff plot for DNF-BSA interaction.

3.3. Energy transfer and binding distance between DNF and BSA

Fluorescence resonance energy transfer (FRET) is a physical phenomenon that is widely used to study the energy transfer between a donor molecule and an acceptor molecule with a distance (r) of 10-100 Å. FRET, as a distance-dependent process, occurs when there is enough overlap between the emission spectrum of the donor and the absorption spectrum of the acceptor molecules [6, 26].

To evaluate the spectral overlap and FRET between BSA and DNF at 298 K, the following equations (Eq. 6-8) were applied [34, 35]:

$$E = 1 - \frac{F}{F_0} = \frac{R_0^6}{R_0^6 + r_0^6}$$

(6)

where, F and F_0 are the emission intensities of the BSA (donor) with and without DNF (acceptor), respectively. R_0 (nm) and r_0 (nm) denote the critical distance at which 50% of energy can transfer from the donor to the acceptor (which is obtained using Eq. 7) and the distance between BSA and DNF, respectively.

$$R_0^6 = 8.79 \times 10^{-25} K^2 n^{-4} \Phi J$$

(7)

where spatial orientation factors between the donor (BSA) and the acceptor (DNF) and the medium's refractive index, are K^2 and n, respectively. The emission quantum yield of the BSA (Φ) and the
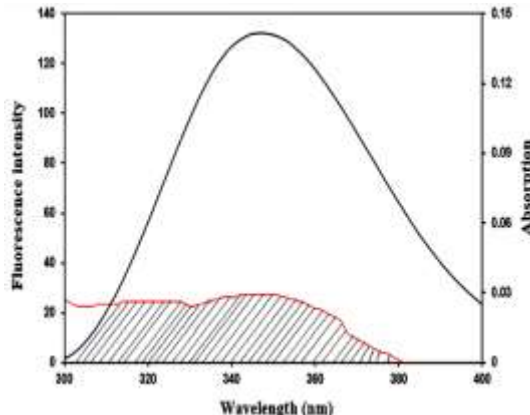
spectral overlap between BSA and DNF (J; $M^{-1}cm^{-1}nm^4$) are represented in Eq.7. Equation 8 can be used to get the J factor's value:

$$J = \frac{\int_0^\infty F(\lambda)\varepsilon(\lambda)\lambda^4 d\lambda}{\int_0^\infty F(\lambda)d\lambda}$$

(8)

where, $F(\lambda)$ and $\varepsilon(\lambda)$ are the emission intensity of BSA and the extinction coefficient of the DNF at wavelength λ, respectively. The constant values in the equations above assume nm units for both λ and R_0, as well as $M^{-1}cm^{-1}$ units for $\varepsilon(\lambda)$.

The overlaps between the absorption spectrum of DNF and the emission spectrum of BSA are shown in Fig. 8. Equations 6-8 were used to calculate the r value, and the results are reported in Table 3. The distance between the BSA–DNF complex was found to be in the range of 10–100 nm, validating the energy transfer from BSA to DNF.

The obtained data from the investigation of the mode of binding between DNF and BSA, i.e. the K_{SV}, k_q, K_a, K_b, n, ΔG, ΔS, ΔH, and R values, is in good agreement with those reported in the literature for various fluoroquinolones [36-38].

Fig. 8. Spectral overlap between the emission spectrum of BSA (2.0×10^{-6} M) and the absorption spectrum of DNF (2.0×10^{-6} M).

**Table 3.** FRET parameters calculated for BSA–DNF system.

System	J (M^{-1}cm^{-1}nm^4)	R_0 (nm)	r (nm)	E_{FRET}
BSA-DNF	1.73×10^{13}	2.2	2.1	0.498

3.4. Molecular docking results

Molecular docking studies were carried out to investigate the binding interaction between DNF and BSA and analyze the binding sites of DNF on BSA. Molecular docking outputs revealed that DNF binds with a high affinity to the hydrophobic cavity between domain II and domain III (Fig 9). Also, results indicated that hydrogen bonding plays a main role in complex formation between

BSA and DNF. The BSA-DNF complex is surrounded by several amino acid residues. Among them, His 145, Asp 108, and Arg 458 bind to DNF through hydrogen bonding, and Ala 193, Arg 196, Ser 192, and Leu 189 interact with DNF by hydrophobic interactions (alkyl hydrophobic and mixed pi/alkyl hydrophobic interactions). The value of ΔG calculated from docking simulation was -6.71 Kcal.mol^{-1}. The observed difference

between the theoretically obtained (-28.18 kJ.mol^{-1}) and experimentally determined ΔG values (-27.67 kJ.mol^{-1}) may be attributed to the lack of water molecules (solvent), the rigidity of other receptor BSA in the *in silico* studies, and the buffer effects. Also, the obtained results showed that hydrogen bonds play an important role in complex formation between DNF and BSA. The intermolecular energy, internal energy, and inhibition constant calculated from molecular docking studies were -6.36 kcal.mol^{-1}, 0.03 kcal.mol^{-1} and 145.94 μM, respectively.
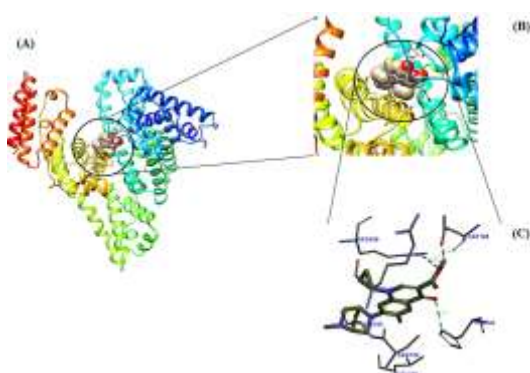
Fig. 9. Molecular docking results of binding of DNF on BSA (A) and binding details of the interaction of DNF with BSA (B) and (C).

4. CONCLUSION

In this work, the interaction of danofloxacin (DNF) with bovine serum albumin (BSA) was studied by the use of some spectroscopic techniques including UV-Vis absorption and fluorescence spectroscopies, and molecular docking modeling. Different binding parameters including k_q, K_{sv}, K_a, K_b, and n values were estimated using fluorometric data analysis. Fluorescence studies revealed that DNF binds to BSA and efficiently quenches BSA intrinsic emission via a static quenching manner. Static quenching was dominant in this research, as evidenced by the linearity of Stern-Volmer graphs in the desired concentration range, very high values of k_q relative to the dynamic quenching constant of the biomolecule, and decreasing K_{sv} values with rising temperature. Also, UV-Vis absorption spectra of BSA in the presence of DNF showed that binding of DNF to BSA does not cause significant conformational changes in BSA secondary structure. The thermodynamic parameters were calculated and the signs of these parameters indicated that DNF-BSA complex formation is a spontaneous process and van der Waals forces and hydrogen bonding are important in the establishment of the DNF-BSA complex. FRET determined a distance of 2.1 nm between the donor (BSA) and acceptor (DNF), indicating that energy transfer had occurred between them. The molecular docking results were successfully employed for a detailed analysis of BSA binding sites, and the experimental results of the spectroscopic approaches were corroborated. This type of drug-protein interaction research is believed to be valuable in the fields of life sciences, chemistry, clinical medicine, and the pharmaceutical industry.

REFERENCES

[1] R. Choudhury, S.R. Patel, and A. Ghosh, Selective detection of human serum albumin by near-infrared emissive fluorophores: Insights into structure-property relationship, *J. Photochem. Photobiol. A Chem.* 376 (2019) 100-107.

[2] S. Paul, N. Sepay, S. Sarkar, P. Roy, S. Dasgupta, P. Saha Sardar, and A. Majhi, Interaction of serum albumins with fluorescent ligand 4-azido coumarin: Spectroscopic analysis and molecular docking studies, *New J. Chem.* 41 (2017) 15392–15404.

[3] M. Shaghaghi, G. Dehghan, S. Rashtbari, N. Sheibani, and A. Aghamohammadi, Multispectral and computational probing of the interactions between sitagliptin and serum albumin, *Spectrochim. Acta A Mol. Biomol. Spectrosc.* 223 (2019) 117286.

[4] H. Zhang, H. Deng, and Y. Wang, Comprehensive investigations about the binding interaction of acesulfame with human serum albumin, *Spectrochim. Acta A Mol. Biomol. Spectrosc.* 237 (2020) 118410.

[5] H. Tang, L. Huang, D. Zhao, C. Sun, and P. Song, Interaction mechanism of flavonoids on bovine serum albumin: Insights from molecular property-binding affinity relationship, *Spectrochim. Acta A Mol. Biomol. Spectrosc.* 239 (2020) 118519.

[6] M. Shaghaghi, S. Rashtbari, S. Vejdani, G. Dehghan, A. Jouyban, and R. Yekta, Exploring the interactions of a Tb (III)–quercetin complex with serum albumins (HSA and BSA): spectroscopic and molecular docking studies, *Luminescence* 35 (2020) 512-524.

[7] D. Ghosh, Kaushik; Rathi, Sweety; and Arora, Fluorescence spectral studies on the interaction of fluorescent probes with Bovine Serum Albumin (BSA), *J. Lumin.* 175 (2016) 135–140.

[8] K.A. Majorek, P.J. Porebski, A. Dayal, M.D. Zimmerman, K. Jablonska, A.J. Stewart, M. Chruszcz, W. Minor, Structural and immunologic characterization of bovine, horse, and rabbit serum albumins, *Mol. Immunol.* 52 (2012) 174-182.

[9] P. Sengupta, P.S. Sardar, P. Roy, S. Dasgupta, and A. Bose, Investigation on the interaction

of Rutin with serum albumins: Insights from spectroscopic and molecular docking techniques, *J. Photochem. Photobiol. A Chem.* 183 (2018) 101-110.

[10] D. Velic, C. Charlier, M. Popova, T. Jaunet-Lahary, Z. Bouchouireb, S. Henry, P. Weigel, J.Y. Masson, A. Laurent, I. Nabiev, F. Fleury, Interactions of the Rad51 inhibitor DIDS with human and bovine serum albumins: Optical spectroscopy and isothermal calorimetry approaches, *Biochimie.* 167 (2019) 187-197.

[11] A. Shamsi, T. Mohammad, S. Anwar, M.F. Alajmi, A. Hussain, M.I. Hassan, F. Ahmad, A. Islam, Probing the interaction of Rivastigmine Tartrate, an important Alzheimer's drug, with serum albumin: Attempting treatment of Alzheimer's disease, *Int. J. Biol. Macromol.* 148 (2020) 533-542.

[12] B.X. Huang, H.-Y. Kim, and C. Dass, Probing the three-dimensional structure of bovine serum albumin by chemical cross-linking and mass spectrometry, *J. Am. Soc. Mass Spectr.* 15 (2004) 1237-1247.

[13] X. Xiong, J. He, H. Yang, P. Tang, B. Tang, Q. Sun, H. Li, Investigation on the interaction of antibacterial drug moxifloxacin hydrochloride with human serum albumin using multi-spectroscopic approaches, molecular docking and dynamical simulation, *Rsc Adv.* 7 (2017) 48942-48951.

[14] J.-h. Shi, D.-q. Pan, M. Jiang, T.-T. Liu, and Q. Wang, Binding interaction of ramipril with bovine serum albumin (BSA): insights from multi-spectroscopy and molecular docking methods, *J. Photochem. Photobiol. B Biol.* 164 (2016) 103-111.

[15] Q. Wang, C. Huang, M. Jiang, Y. Zhu, J. Wang, J. Chen, and J. Shi, Binding interaction of atorvastatin with bovine serum albumin: Spectroscopic methods and molecular docking, *Spectrochim. Acta A Mol. Biomol. Spectrosc.* 156 (2016) 155–163.

[16] R. Patel, F.A. Wani, F. Mahfooz, P. Mishra, and M.A. Siddiquee, Interaction of human serum albumin with diclofenac incorporated in catanionic vesicles, *Mater. Today: Proc.* 36 (2021) 736-742.

[17] D. Terrado-Campos, K. Tayeb-Cherif, J. Peris-Vicente, S. Carda-Broch, and J. Esteve-Romero, Determination of oxolinic acid, danofloxacin, ciprofloxacin, and enrofloxacin in porcine and bovine meat by micellar liquid chromatography with fluorescence detection, *Food chem.* 221(2017) 1277-1284.

[18] F.S. Aliabadi, M.F. Landoni, and P. Lees, Pharmacokinetics (PK), pharmacodynamics (PD), and PK-PD integration of danofloxacin in sheep biological fluids, *Antimicrob. Agents Chemother.* 47 (2003) 626-635.

[19] S.R. Han, J.Yu, and S.-W. Lee, In vitro selection of RNA aptamers that selectively bind danofloxacin, *Biochem. Biophys. Res. Commun.* 448 (2014) 397-402.

[20] Y. Yang, Y. Zhang, J. Li, P. Cheng, T. Xiao, I. Muhammad, H. Yu, R. Liu, X. Zhang, Susceptibility breakpoint for danofloxacin against swine Escherichia coli," *BMC Vet. Res.* 15 (2019) 1-9.

[21] M. ud din Parray, M.U.H. Mir, N. Dohare, N. Maurya, A.B. Khan, M.S. Borse, R. Patel, Effect of cationic gemini surfactant and its monomeric counterpart on the conformational stability and esterase activity of human serum albumin, *J. Mol. Liq.* 260 (2018) 65-77, 2018.

[22] F. Nasiri, G. Dehghan, M. Shaghaghi, S. Datmalchi, and M. Iranshahi, Probing the interaction between 7-geranyloxycoumarin and bovine serum albumin: Spectroscopic analyzing and molecular docking study, *Spectrochim. Acta A Mol. Biomol. Spectrosc.* 254 (2021) 119664.

[23] S. Rashtbari, G. Dehghan, R. Yekta, A. Jouyban, and M. Iranshahi, Effects of resveratrol on the structure and catalytic function of bovine liver catalase (BLC): spectroscopic and theoretical studies, *Adv.Pharm. Bull.* 7 (2017) 349-357.

[24] M. Sharifi, J.E.N. Dolatabadi, F. Fathi, M. Rashidi, B. Jafari, H. Tajalli, and M.-R. Rashidi, Kinetic and thermodynamic study of bovine serum albumin interaction with rifampicin using surface plasmon resonance and molecular docking methods, *J. Biomed. Optics* 22 (2017) 1–6.

[25] N. Dohare, A.B. Khan, F. Athar, S.C. Thakur, and R. Patel, Urea-induced binding between diclofenac sodium and bovine serum albumin: a spectroscopic insight, *Luminescence* 31 (2016) 945-951.

[26] S. Rashtbari, S. Khataee, M. Iranshahi, A.A. Moosavi-Movahedi, G. Hosseinzadeh, and G. Dehghan, Experimental investigation and molecular dynamics simulation of the binding of ellagic acid to bovine liver catalase: Activation study and interaction mechanism, *Int. J. Biol. Macromol.* 143 (2020) 850-861.

[27] S. Rashtbari, G. Dehghan, R. Yekta, and A. Jouyban, Investigation of the binding mechanism and inhibition of bovine liver catalase by quercetin: Multi-spectroscopic and computational study, *Bioimpacts: Bi* 7 (2017) 147-153.

[28] S.T.N. G.G. Ariga, P.N. Naik, and S.A. Chimatadar, Interactions between epinastine and human serum albumin: investigation by

fluorescence, UV–vis, FT–IR, CD, lifetime measurement and molecular docking, *J. Mol. Struct.* 1137 (2017) 485–494.

[29] C.-Y. Liang, J. Pan, A.-M. Bai, and Y.-J. Hu, Insights into the interaction of human serum albumin and carbon dots: Hydrothermal synthesis and biophysical study, *Int. J. Biol. Macromol.* 149 (2020) 1118-1129.

[30] R. Yekta, G. Dehghan, S. Rashtbari, R. Ghadari, and A.A. Moosavi-Movahedi, The inhibitory effect of farnesiferol C against catalase; Kinetics, interaction mechanism and molecular docking simulation, *Int. J. Biol. macromol.* 113 (2018) 1258-1265.

[31] G. Dehghan, S. Rashtbari, R. Yekta, and N. Sheibani, Synergistic inhibition of catalase activity by food colorants sunset yellow and curcumin: An experimental and MLSD simulation approach, *Chem-Biol.Interact.* 311 (2019) 108746.

[32] T.A. Wani, A.H.Bakheit. A. A.Al-Majed, N. Altwaijry, A. Baquaysh, A. Aljuraisy, and S. Zargar, Binding and drug displacement study of colchicine and bovine serum albumin in presence of azithromycin using multispectroscopic techniques and molecular dynamic simulation, *J. Mol. Liq.* 333 (2021) 115934.

[33] L. Khalili and G. Dehghan, A comparative spectroscopic, surface plasmon resonance, atomic force microscopy and molecular docking studies on the interaction of plant derived conferone with serum albumins, *J. Lumin.* 211 (2019) 193–202.

[34] A. Hasanzadeh, G. Dehghan, M. Shaghaghi, Y. Panahi, A. Jouyban, and R. Yekta, Multispectral and molecular docking studies on the interaction of human serum albumin with iohexol, *J. Mol. Liq.* 248 (2017) 459-467.

[35] A. Sarnejad, M. Shaghaghi, G. Dehghan, and S. Soltani, Binding of carvedilol to serum albumins investigated by multi-spectroscopic and molecular modeling methods, *J. Lum.* 176 (2016) 149-158.

[36] Y. Ni, S. Su, and S. Kokot, Spectrometric studies on the interaction of fluoroquinolones and bovine serum albumin, *Spectrochim. Acta A Mol. Biomol. Spectrosc.* 75 (2010) 547-552.

[37] Y.J. Hu, Y.O.Yang, A.M. Bai, W. Li, and Y. Liu, Investigation of the interaction between ofloxacin and bovine serum albumin: spectroscopic approach, *J. Solution. Chem.* 39 (2010) 709-717.

[38] N.Seedher, P.Agrawal, Complexation of fluoroquinolones antibiotics with human serum albumin: A fluorescence quenching study, *J. Lumin.* 130 (2010) 1841-1848.

[39] S.Q. Lian, J. Lian, G.R. Wang, L. Li, D.Z. Yang, and Y.S. Xue, Investigation of binding between fluoroquinolones and pepsin by fluorescence spectroscopy and molecular simulation, *Luminescence* 34 (2019) 595-601.
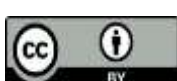
برهمکنش های مولکولی دانوفلوکساسین با آلبومین سرم گاوی: یک بررسی تجربی و تئوری

معصومه شقاقی*[۱]، سمانه رشت بری[۲]، لاله سلوکی[۱]، سمیه سلطانی[۳، ۴]، غلامرضا دهقان[۲]

۱. گروه شیمی، دانشگاه پیام نور، صندوق پستی ۴۶۹۷-۱۹۳۹۵ تهران، ایران

۲. گروه زیست‌شناسی، دانشکده علوم طبیعی، دانشگاه تبریز، تبریز، ایران

۳. مرکز تحقیقات آنالیز دارویی، دانشگاه علوم پزشکی تبریز، تبریز، ایران

۴. دانشکده داروسازی، دانشگاه علوم پزشکی تبریز، تبریز، ایران

چکیده

دانوفلوکساسین (DNF)، یک فلوروکینولون مصنوعی، به طور گسترده‌ای به عنوان یک عامل ضد باکتری در برابر طیف گسترده‌ای از عوامل بیماری زا استفاده می‌شود. در مطالعه حاضر، اثرات دانوفلوکساسین بر ساختار آلبومین سرم گاوی (BSA) با استفاده از تکنیک‌های طیف‌سنجی جذبی UV-Vis و فلوئورسانس و روش‌های داکینگ مولکولی در دماهای مختلف مورد بررسی قرار گرفت. نتایج به‌دست‌آمده از مطالعات جذب UV-Vis نشان داد که ریزمحیط باقی‌مانده‌های فلوروفور پس از برهم‌کنش با دانوفلوکساسین تغییر قابل‌توجهی نمی‌کند. همچنین، مطالعات فلورومتری تشکیل کمپلکس BSA-DNF و خاموش‌شدن فلوئورسانس آلبومین سرم گاوی را در حضور دانوفلوکساسین نشان داد. تعداد محل‌های اتصال و ثابت‌های اتصال به ترتیب ۱~ و در مرتبه ۱۰۳ محاسبه شد. با توجه به پارامترهای ترمودینامیکی، نیروهای واندروالسی و پیوند هیدروژنی نقش اصلی را در تشکیل کمپلکس BSA-DNF ایفا می‌کنند که یک فرآیند خود به خودی می‌باشد.. فاصله اتصال بین دانوفلوکساسین و آلبومین سرم گاوی با روش انتقال انرژی تشدید فورستر محاسبه شد. نتایج داکینگ مولکولی با داده‌های ترمودینامیکی و طیف‌سنجی مطابقت داشت و مکانیسم اتصال دانوفلوکساسین به آلبومین سرم گاوی را تأیید کرد.